



Potassium Fractionation and Stock in Clay Soils: Influence of Geochemical and Mineralogical Properties in Yogyakarta Region, Indonesia

Eko Hanudin^{1*}, Padana Aperta Barus², Makruf Nurudin¹ and Sri Nuryani Hidayah Utami¹

¹Department of Soil Sciences, Faculty of Agriculture, Universitas Gadjah Mada, Yogyakarta, Indonesia;

²National Research and Innovation Agency (BRIN), Bogor, Indonesia

*Corresponding author: ekohanudin@ugm.ac.id

Abstract

Research on potassium (K) dynamics in upland clay soils, particularly those derived from tertiary-aged rocks, remains limited in Yogyakarta. This study aimed to investigate the relationships among geochemical indices, K fractions, and K stock in upland clay soils, considering the influence of their physical, chemical, and mineralogical properties. Thirty soil samples were collected from five geological formations at two depths (0 to 20 and 20 to 40 cm), with three replicates selected from each formation through purposive sampling. Soil characterization was performed using routine methods, energy-dispersive X-ray fluorescence (EDXRF), and X-ray diffraction (XRD) analyses. Geochemical indices such as the chemical index of alteration (CIA), Vogt residual index (VR), alumina to potassium oxide ratio (AKN), silica to sesquioxide (Si/Seq), and Ruxton ratio (R) were calculated, and K stock was determined. The results showed that feldspar contributes to K stock in upland clay soils. Spearman's correlation analysis revealed that only the AKN index significantly correlated with K-pseudo-total and K-non-exchangeable ($p < 0.01$). The highest K-pseudo-total concentration was found in P4-Sentolo (1,326 to 1,715 mg kg⁻¹) and the highest concentrations of K-non-exchangeable were observed in P5-Kebobutak (1.37 to 1.78 cmolc kg⁻¹). Significant correlations between K-exchangeable and K-water-soluble with total organic carbon and K-non-exchangeable were also identified ($p < 0.01$). The highest K-exchangeable concentration was recorded in P2-Nglanggran (0.17 to 0.33 cmolc kg⁻¹), while the lowest was found in P1-Wonosari (0.04 to 0.09 cmolc kg⁻¹). All clay soils exhibited K-exchangeable concentrations below the critical deficiency level. Understanding these relationships is crucial for effective soil management and sustainable agricultural production. Targeted fertilization strategies can be developed based on the dominant K fraction in each soil.

Keywords: feldspars; geochemical indices; geological formations; K fractions; upland clay soils

Cite this as: Hanudin, E., Barus, P. A., Nurudin, M., & Utami, S. N. H. (2025). Potassium Fractionation and Stock in Clay Soils: Influence of Geochemical and Mineralogical Properties in Yogyakarta Region, Indonesia. *Caraka Tani: Journal of Sustainable Agriculture*, 40(2), 156-172. doi: <http://dx.doi.org/10.20961/carakatani.v40i2.93721>

INTRODUCTION

Potassium (K) is a primary macronutrient that plants require in large quantities. It plays a vital role in plant growth, influencing physiological functions such as cellular growth and wood formation, water content and movement in the xylem and phloem, nutrient and metabolite transport, and stress responses (Sardans and

Peñuelas, 2021). Potassium also contributes to plant health by enhancing resistance to biotic and abiotic stresses, including diseases, pests, drought, salinity, cold, frost, and waterlogging (Zörb et al., 2014; Hasanuzzaman et al., 2018). Adequate K supply maintains photosynthesis and can boost off-season production of high-

* Received for publication September 24, 2024

Accepted after corrections January 18, 2025

quality fruits (Maier et al., 2022; Babla et al., 2023). Irawan and Putra (2020) found that K supplementation improved the anatomical development of oil palm seeds, including xylem, phloem, and cortex cells while enhancing drought tolerance.

In nature, K is primarily supplied through weathering primary minerals in rocks. It is one of the most abundant plant nutrients, accounting for 2.6% in the earth's crust. On average the soil constitutes 0.04 to 3% K, but most of the K^+ in the soil is incorporated in the crystal lattice structure of minerals and is not directly available for plant uptake (Demidchik et al., 2014). The main K-bearing minerals in soils are feldspar, mica, biotite, muscovite, and nepheline, with feldspar and mica constituting 90 to 98% of soil K deposits (Rawat et al., 2017; Soumare et al., 2023). In phyllosilicate clays, illite, a type of clay mica, is the dominant high-charge, K-bearing mineral. Weathering of illite may transform it into vermiculite, reducing charge and facilitating the release of K. Han et al. (2019) reported that artificial submergence accelerates the breakdown of K-bearing minerals, converting K-lattice-bound into K-non-exchangeable, thereby improving K availability. Potassium in the minerals' core interlayers (i-positions) is typically unavailable to plants unless exposed to rhizosphere conditions (Bell et al., 2021). Plant residues decomposing into soil organic matter can also contribute to K availability by increasing K-exchangeable levels (Han et al., 2023).

Potassium dynamics in soil are often linked to physicochemical properties and mineralogy (Han et al., 2021; Jindaluang and Darunsontaya, 2023). Geochemical indices, derived from the molar ratios of soil elements obtained through X-ray fluorescence (XRF) analysis, are less frequently used but can offer valuable insights into K dynamics. These indices are commonly employed to estimate soil weathering and the intensity of mineral weathering (Fiantis et al., 2017; 2021; Heidari et al., 2022). Geochemical indices thus provide a complementary perspective on K dynamics, especially in soils with varying parent materials and mineralogy.

Potassium is commonly classified into five fractions based on its availability to plants: K-water-soluble (K-water-sol), K-exchangeable (K-exch), K-non-exchangeable (K-non-exch), K-lattice, and total K (Pathariya et al., 2022). These fractions exist in dynamic equilibrium, influenced by soil properties, mineral composition, and weathering intensity. The K-

exch and K-non-exch distribution varies depending on the soil's parent material and texture (Akbas et al., 2017). Studies in Japan have shown that K-non-exch is particularly significant in lowland soils (including paddy soils, gley lowland soils, gray lowland soils, and brown lowland soils), upland soils (gray upland soils and brown forest soils), and red-yellow soils (red and yellow soils) with high contributions from phyllosilicates like mica and vermiculite (Kitagawa et al., 2018).

In contrast, Andosols (Wet Andosols, Non-allophanic Andosols, and Andosols) and Volcanogenous Regosols have relatively low K-non-exch contributions. In Indonesia, K fractionation was measured by Nursyamsi et al. (2008) on lowland clay soils containing smectite in Java. The results indicated that the content of K-water-sol, K-exch, K-non-exch, and total K followed the order of Vertisols > Alfisols > Inceptisols. Moreover, the percentage distribution of soil K fractions was in the order of K-water-sol < K-exch < K-non-exch. Despite the high total K content, most of it was in the non-exchangeable fraction, rendering it slowly available for plant growth.

Research on K fractionation in clay soils, particularly in upland areas derived from tertiary-aged rocks, remains scarce in Indonesia. Existing studies mainly focus on K-exch, with limited attention to the role of K-non-exch and its relationship with soil mineralogy. Recent findings also indicate K deficiencies in rice and maize crops in intensively cultivated areas of Central and East Java (Rizzo et al., 2024). Understanding K dynamics is essential for evaluating K nutrient availability and developing effective K fertilizer recommendations to address deficiencies and support sustainable agricultural productivity.

This study aims to 1) analyze various K fractions in upland clay soils using a non-sequential technique (K-pseudo-total, K-lattice, K-non-exch, exchangeable K^+ , and K-water-sol), 2) investigate how different parent materials (clay sediment, weathered limestone, weathered volcanic breccia, weathered tuff, and altered volcanic ash) influence the content and distribution of K fractions, and 3) explore the relationship between soil weathering and K fractions through several geochemical indices such as the chemical index of alteration (CIA), Vogt residual index (VR), alumina to potassium oxide ratio (AKN), silica to sesquioxide (Si/Seq), and Ruxton ratio (R). By addressing these objectives, this study seeks to enhance

our understanding of K dynamics related to soil mineralogy and parent material, contributing to the broader knowledge of soil fertility management, particularly in tropical regions with complex parent material variability.

MATERIALS AND METHOD

Study area

The field research was conducted at five locations based on geological formations within the administrative region of the Special Region of Yogyakarta (Figure 1). At each location, morphological description and sample collections were conducted at three observation points as replications, resulting in a total of 15 observation points. The observation points were selected using a purposive sampling method, with an emphasis on similarities in topography, soil color, and land use. This approach was employed to obtain pedons with nearly identical characteristics, ensuring they represented the condition of soils formed over specific geological formations. The topography of all locations is hilly, and the observation points are situated on the summits of the hills. The descriptions of these five locations are provided in Table 1.

The average annual rainfall in the study area is approximately 2,422 mm year⁻¹ (BBSDLP, 2017a; 2017b). The study area is categorized as type C (moderately humid) according to the Smith-Fergusson climate system. Based on the Köppen climate system, it is classified as a tropical monsoon (Am).

Soil chemical and mineralogical analysis

Soil observations and sample collection were conducted by digging mini-pits with dimensions of 50 cm x 80 cm x 50 cm. Soil samples were taken from two layers at 0 to 20 cm and 20 to 40 cm depths, representing the root zone and nutrient uptake areas. Both disturbed and undisturbed soil samples were collected for laboratory analysis. All samples were kept in plastic bags and sent shortly to the laboratory for analysis. Undisturbed soil samples were air-dried to achieve stable moisture content. Coarse fragments and visible roots were removed. Then, air-dried soil samples were grounded and sieved to a fine earth size ($\emptyset < 2$ mm). Soil physical properties such as bulk density and soil texture were determined using the core and pipette methods, respectively (van Reeuwijk, 2002). Total organic carbon was determined by the combustion method using a Leco EA CN 628 series. Soil pH was measured in H₂O (1:2.5) using a digital pH meter (Horiba LAQUAact D-74). Cation exchange capacity (CEC) and exchangeable cations were analyzed by extracting 10 g soil with 50 ml 1 N NH₄OAc pH 7 (van Reeuwijk, 2002). The CEC for the clay fraction (CEC_{clay}) was calculated by dividing the CEC by the clay percentage.

K-pseudo-total content was determined by wet digestion (H₂SO₄ + HClO₄) (Rao et al., 2011). K-exch was determined by extraction with 1 N NH₄OAc pH 7 (Van Reeuwijk, 2002). K-non-exch was measured after boiling in 1 N HNO₃. Water-soluble K (K-water-sol) was determined

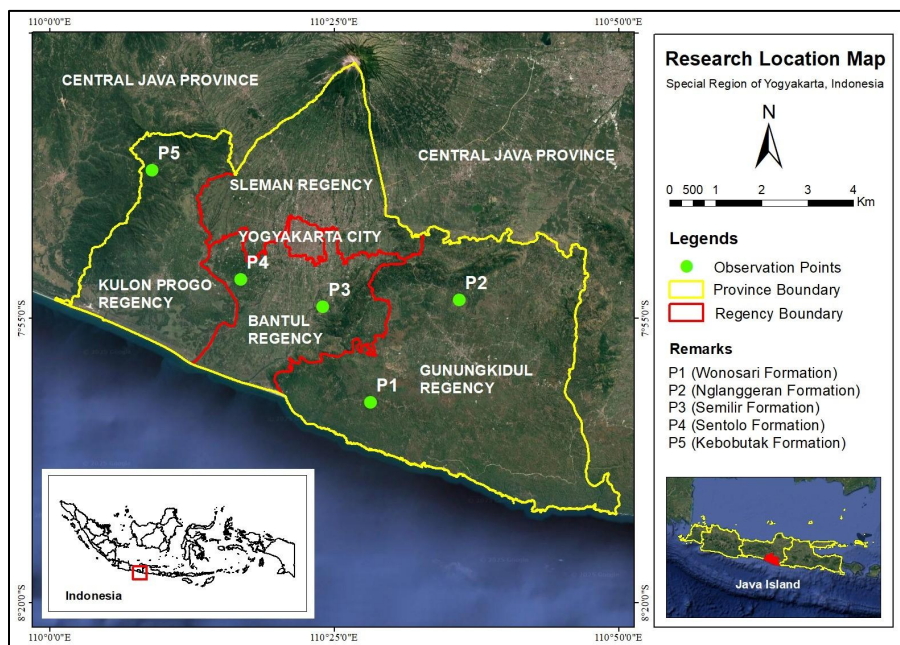


Figure 1. Location of mini pits in the study area

Table 1. Description of the locations of the five pedons

Pedon	Bedrock*	Parent material	Soil order	Vegetation	Longitude/ Latitude
P1- Wonosari	Limestone	Transported clay sediment	Alfisols	Teak (<i>Tectona grandis</i>)	110°28'21.6" E 8°02'23.7" S
P2- Nglanggran	Tertiary volcanic breccia	Weathered volcanic breccia	Inceptisols	Teak (<i>Tectona grandis</i>), <i>Albizia chinensis</i>)	110°35'59.7" E 7°53'36.2" S
P3-Semilir	Tertiary tuff	Weathered tuff breccia	Entisols	Teak (<i>Tectona grandis</i>)	110°23'51.8" E 7°54'11.6" S
P4-Sentolo	Limestone	Weathered limestone	Vertisols	Teak (<i>Tectona grandis</i>)	110°16'30.6" E 7°51'28.4" S
P5- Kebobutak	Tertiary breccia	Altered volcanic material	Inceptisols	<i>Albizia chinensis</i> , Mahogany (<i>Swietenia mahagoni</i>)	110°08'53.5" E 7°41'56.4" S

Note: *Based on Rahardjo et al. (1995) and Surono et al. (1992)

in 1:5 soil-water suspension after shaking for two hours and allowing it to stand overnight (Harsha and Jagadeesh, 2017). All the extracted filtrate from each K fraction was measured using a flame photometer. In addition, the K-lattice was estimated based on the difference between total K and the sum of exchangeable, non-exchangeable and water-soluble K. Calculation of K stock was based on formula: $K_{stock} = K_d \times \rho \times \% K_{tot}$ (modified from Kauer et al., 2021), where: K_{stock} = K stock in soil (ton ha⁻¹), K_d = layer depth (cm), ρ = bulk density (g cm⁻³), and K_{tot} = K-pseudo-total (mg kg⁻¹).

The elemental composition of soil samples was measured using energy-dispersive X-ray fluorescence (EDXRF). Concentrations of elemental oxides were determined using pressed pellet samples prepared following procedures outlined by Tavares et al. (2019). Fine soil particles (< 2 mm) were initially dried at 105 °C for 24 hours, then ground in a planetary ball mill using a tungsten carbide jar and 10 tungsten carbide balls. Grinding was performed at a speed of 400 rpm for 10 minutes. The ground and homogenized samples were transferred to an aluminum cup and pressed using a hydraulic

press. The pellet samples were scanned using the EDXRF spectrometer Bruker S2 PUMA Series 2. For loss-on-ignition (LOI) measurement, 1 g of the ground sample was transferred to alumina crucibles and heated at 550 °C for 1 hour, followed by an increase to 950 °C for 2 hours. After cooling, the crucibles were reweighed to determine the $\%LOI = \frac{W_2 - W_3}{W_2 - W_1} \times 100\%$, where W_1 = weight of crucible, W_2 = weight of crucible + oven dry sample, and W_3 = weight of crucible + oven dry sample after ignition.

Five geochemical indices were determined, and the details of the formulas and the relevant references are given in Table 2. The CIA estimates the weathering intensity. VR assesses the maturity of residual sediments. The ratio of AKN reflects the alteration of feldspar. The Si/Seq indicates the degree of desilication. The R relates to the loss of silica compared to the total loss of alumina, with alumina considered immobile during weathering.

The mineralogy of bulk soil was determined by X-ray Diffraction (XRD) analysis. Bulk samples were pulverized into a powder and passed through a 100- μ m sieve. The powdered samples were

Table 2. Geochemical indices determined in the present study

Index	Formula	Reference
CIA (Mole ratio)	$[(Al_2O_3/Al_2O_3 + CaO + Na_2O + K_2O)] \times 100$	Nesbitt and Young (1984)
VR (Mole ratio)	$(Al_2O_3 + K_2O)/(MgO + CaO + Na_2O)$	Roadset (1972)
AKN (Oxide ratio)	$Al_2O_3/(K_2O + Na_2O)$	Harnois and Moore (1988)
Si/Seq (Mole ratio)	$SiO_2/(Al_2O_3 + Fe_2O_3)$	Moignien (1966)
R (Mole ratio)	SiO_2/Al_2O_3	Ruxton (1968)

Note: CIA = Chemical index of alteration, VR = Vogt residual index, AKN = Alumina to potassium oxide ratio, Si/Seq = Silica to sesquioxide, R = Ruxton ratio

carefully spread evenly on a sample holder cavity. The unoriented mounts of fine powders were analyzed using a Rigaku Ultima IV with $\text{CuK}\alpha$ radiation target, operated at 40 kV and 30 mA. Specimens were scanned from 3° to 60° 2θ at a rate of 3° m^{-1} . The diffraction patterns were analyzed qualitatively and quantitatively using the Rietveld BGMN model available in PROFEX 5.2.4 software.

Data analysis

The data were described using the mean value. A two-way analysis of variance (ANOVA) procedure was conducted to test the impact of parent material and depth on K fraction and K stock. The normality test showed that the data were not normally distributed. Therefore, the Spearman correlation was used to analyze the relationships between soil properties, geochemical indices, and the concentrations of K fractions. Correlations were considered statistically significant at a probability level of 5% or less ($p < 0.05$). All statistical analyses used R-studio software (R Core Team, 2020).

RESULTS AND DISCUSSION

Mineralogy and geochemical conditions of soil

The mineralogy of bulk samples from the studied soils is presented in Table 3. P1-Wonosari was dominated by 1:1 minerals, with minor amounts of goethite and hematite. Calcite was not observed in P1-Wonosari, indicating that the soil did not develop from the Wonosari limestone but rather from clay sediments (Mulyanto, 2022). P2-Nglanggran was also dominated by 1:1 minerals, with smaller amounts of goethite, quartz, and maghemite. P3-Semilir consists of nearly equal proportions of 1:1 and 2:1 minerals, along with smaller amounts of quartz and maghemite. Unlike the other soils, the mineralogy of P4-Sentolo is more diverse. The dominant

minerals in this soil are 2:1 and 1:1 minerals. Calcite, plagioclase, and quartz are present in smaller amounts, with calcite being inherited from weathered limestone. P5-Kebobutak is dominated by 1:1 minerals, with very small amounts of quartz and maghemite. The dominance of 1:1 minerals in P5-Kebobutak is attributed to the alteration of volcanic materials (Sartohadi et al., 2018). Overall, variation exists in the mineral composition of upland clay soils in Yogyakarta.

Among all soils, easily weatherable minerals were identified only in P4-Sentolo (plagioclase). The scarcity of easily weatherable minerals indicated that the upland clay soils had limited nutrient reserves. Plagioclase contained a small amount of K_2O and acted as a source of K in P4-Sentolo. Potassium release occurs through the weathering process (Anda et al., 2015). Common K-bearing minerals in soils, such as feldspar and mica, were not identified by XRD analysis in any of the upland clay soils. Moreover, a significant amount of 2:1 minerals was observed only in P3-Semilir and P4-Sentolo. These 2:1 minerals were likely dominated by expandable clay minerals, such as smectite. The other soils were dominated by 1:1 minerals presumed to be dioctahedral 1:1 clay silicates, such as kaolinite or halloysite. These findings were consistent with mineralogical reports from other soils in adjacent areas near the study site (Sartohadi et al., 2018; Mulyanto, 2022) and other regions (Navarro-Hasse et al., 2023). Furthermore, differences in clay mineralogy had implications for the CEC (Kome et al., 2019). Expandable 2:1 minerals, such as smectite, had a higher negative charge compared to 1:1 clay minerals.

The content of macro-elements was found to vary among soils due to differences in the mineralogy of the parent materials (Tables 4 and 5). The variation in SiO_2 content among soils in this study was not significant (37 to 41%).

Table 3. Mineralogy of bulk samples from the studied soils

Mineral abundance (%)	Sample location and parent materials				
	P1 TCS	P2 WVB	P3 WTB	P4 WLM	P5 AVM
Plagioclase				9	
Hematite	1				
Calcite				10	
Quartz		2	< 1	4	1
Goethite	9	11			
Maghemite		< 1	< 1		1
2:1 group			46	46	
1:1 group	89	86	53	31	98

Note: TCS = Transported clay sediment, WVB = Weathered volcanic breccia, WTB = Weathered tuff-breccia, WLM = Weathered limestone, AVM = Altered volcanic material

However, P3-Semilir and P4-Sentolo, which contain a significant amount of 2:1 minerals, had higher SiO₂ content. The Al₂O₃ content across all soils was also relatively similar (22 to 28%), except for P4-Sentolo, which had significantly lower Al₂O₃ content (16 to 17%). Similarly, the Fe₂O₃ content among the soils was relatively similar (16 to 19%), except for P4-Sentolo (12 to 13%). The behavior of iron in P4-Sentolo contrasted with the findings of Heidari et al. (2022), who observed iron enrichment in soils derived from limestone. The lower Al₂O₃ and Fe₂O₃ content in P4-Sentolo was due to the dilution effect of CaCO₃, reducing the proportion of silicate minerals and iron oxides.

The content of Ca, Mg, and K (expressed as oxides) in all soils was controlled by the mineralogy of the parent materials. The Na₂O content in all soils was very low and below the XRF detection limit, demonstrating that Na has leached out during soil formation. As a monovalent cation, Na⁺ is highly susceptible to weathering and leaching, leaving only a minimal amount in the soil. Furthermore, the highest CaO content was found in P4-Sentolo (11 to 14%), followed by P3-Semilir (1%), P5-Kebobutak, P2-Nglanggran, and P1-Wonosari (0.25 to 0.53%). The exceptionally high CaO content in P4-Sentolo was attributed to the presence of calcite (Kowalska et al., 2021). The highest MgO content was observed in P3-Semilir (2%), followed by P4-Sentolo (1.5%). The lowest MgO content was found in P1-Wonosari (0.3%), followed by P5-Kebobutak (0.3 to 0.4%) and P2-Nglanggran (0.4%). The MgO content in P3-Semilir and P4-Sentolo was higher because both soils contained considerable amounts of 2:1 minerals, as shown by the XRD analysis (Butler et al., 2020).

Surprisingly, the highest average K₂O content was observed in P5-Kebobutak, followed by P4-Sentolo and P2-Nglanggran. In contrast, P3-Semilir and P1-Wonosari contained very low K₂O. The relatively high average K₂O content in P3-Kebobutak and P2-Nglanggran was unexpected, as only P4-Sentolo was identified to contain plagioclase through XRD analysis. K-bearing minerals were likely present in both soils, resulting in higher K₂O content. However, their presence was not detected through XRD analysis of bulk samples.

The elemental composition in all soils showed that mobile elements like Ca, Mg, K, and Na were leached, leaving behind immobile elements (Fe, Al, Ti), except for P4-Sentolo. This occurred because the soils were derived from old tertiary-aged rock that had undergone extensive weathering. Additionally, some of these soils were likely affected by alteration processes, leading to changes in the elemental composition of the parent materials (Pulungan and Sartohadi, 2018; Sartohadi et al., 2018). The low content of soluble macro-elements further emphasized that the clay soils in this study had limited nutrient reserves.

The TiO₂ and MnO contents in all soils ranged from 1.02 to 1.55% and 0.25 to 0.50%, respectively (Table 5). The highest contents were recorded in P2-Nglanggran, while the lowest was found in P4-Sentolo. The P₂O₅ content in P4-Sentolo was very low and undetectable by XRF. The highest P₂O₅ content was identified in P5-Kebobutak, derived from quaternary volcanic ash (0.18 to 0.22%), while the other soils exhibited lower contents (0.09 to 0.17%).

The results of the total element analysis with XRF are very interesting because sulfur (S) elements were found, in addition to the metal

Table 4. Content of Si, Al, K, Ca, Fe, Na, and Mg elements in the studied soils

No. Minipit (Geological formation)	Depth (cm)	Parent materials	SiO ₂	Al ₂ O ₃	K ₂ O	CaO	Fe ₂ O ₃	Na ₂ O	MgO
			----- Wt (%) -----						
P1 (Wonosari)	0–20	TCS	37.23	27.22	0.07	0.40	16.97	nd	0.29
	20–40		38.67	28.46	0.07	0.30	17.31	nd	0.26
P2 (Nglanggran)	0–20	WVB	37.96	25.77	0.23	0.44	18.60	nd	0.40
	20–40		38.25	25.92	0.20	0.36	18.09	nd	0.42
P3 (Semilir)	0–20	WTB	40.06	21.82	0.06	1.23	17.74	nd	2.23
	20–40		40.49	22.46	0.05	1.00	17.73	nd	2.26
P4 (Sentolo)	0–20	WLM	38.83	16.21	0.30	13.54	12.26	nd	1.46
	20–40		41.09	17.13	0.31	11.14	12.54	nd	1.48
P5 (Kebobutak)	0–20	AVM	38.28	27.16	0.37	0.53	15.67	nd	0.36
	20–40		37.15	27.79	0.24	0.25	16.95	nd	0.31

Note: TCS = Transported clay sediment, WVB = Weathered volcanic breccia, WTB = Weathered tuff-breccia, WLM = Weathered limestone, AVM = Altered volcanic material, nd = Not detected

forms as previously described. The S content is expressed in the form of SO_3 (not ionic forms such as SO_4^{2-} or S^{2-}) because the working principle of this tool measures the energy released by atoms when exposed to X-ray radiation. Therefore, the detected S atoms are converted into the SO_3 form, with a more stable chemical bond structure. Sulfur trioxide exhibits a trigonal planar geometry, meaning the sulfur atom is centrally located and surrounded by three oxygen atoms in a flat triangular arrangement with 120-degree bond angles.

The S-O bonds are covalent, involving the sharing of electron pairs. The molecule contains one S=O double bond and two S→O coordinate covalent bonds. The trigonal planar geometry results in high molecular symmetry, minimizing the dipole moment and enhancing stability. The strong covalent bonds between sulfur and oxygen contribute to the molecule's overall stability (Underwood et al., 2014). The SO_3 levels found in the soil at P1 to P5 ranged from 0.08 to 1.0%, except in P3 where it was not detected, and in P4, where it was only 0.04%. The other soils contained relatively similar amounts of SO_3 (0.08 to 0.10%). The macro-element content obtained in this study falls within the range of macro-element content found in clay soils and oxidic soils in tropical regions of Central Africa (Temga et al., 2021).

The comparison of geochemical indices across soils is shown in Table 6. The order of soils from the highest to the lowest CIA (mean values) was P1-Wonosari > P5-Kebobutak > P2-Nglanggran > P3-Semilir > P4-Sentolo. Except for P4-Sentolo, all clay soils had produced CIA values greater than 90. These values were higher than agricultural soils derived from silicate rocks in Europe (Négre et al., 2023). A CIA value greater

than 90 confirmed that the non-calcareous clay soils in this study had undergone intensive weathering. A similar pattern was found in the VR and R indices, but these indices showed a different weathering degree in P3-Semilir compared to the CIA. The VR and R values for P3-Semilir range from 2.78 to 2.98 and 3.06 to 3.12, respectively. These values were typical of moderately weathered soils (Enang et al., 2020). This suggested that Si and Mg leaching in P3-Semilir was less than in other non-carbonate clay soils. The high Si/Seq values also supported this. The low desilication and Mg leaching contributed to the preservation of 2:1 minerals in P3-Semilir.

The AKN values for all soils showed a different trend. The order of AKN values was as follows: P3-Semilir > P1-Wonosari > P2-Nglanggran > P5-Kebobutak > P4-Sentolo. Lower AKN values in P4-Sentolo, P5-Kebobutak, and P2-Nglanggran indicated the presence of feldspar in these soils. The presence of feldspar was not detected through XRD analysis, likely due to being masked by the dominance of clay minerals. It was suggested that the feldspar was contained in the silt fraction (Jindaluang and Darunsontaya, 2023; Volf et al., 2023). Thus, mineral analysis based on particle size was crucial for identifying K_2O sources in clay soils. P5-Kebobutak had relatively low AKN values and contained K_2O similar to P4-Sentolo, which was attributed to the presence of feldspar. The weathered feldspars were also found in other soils derived from altered volcanic material (Pulungan and Sartohadi, 2018; Sartohadi et al., 2018).

This study showed that upland clay soils from various parent materials have distinct geochemical indices, reflecting their mineral content. Soils from clay sediments (P1-Wonosari) had high AKN and Si/Seq values, while carbonate

Table 5. Content of Ti, Mn, P, S, and LOI elements in the studied soils

No. Minipit (Geological formation)	Depth (cm)	Parent materials	TiO ₂	MnO	P ₂ O ₅	SO ₃	LOI
			-----	Molecular proportion (%)			
P1 (Wonosari)	0–20	TCS	1.23	0.31	0.11	0.09	16.08
	20–40		1.23	0.29	0.09	0.08	13.25
P2 (Nglanggran)	0–20	WVB	1.55	0.50	0.17	0.09	14.29
	20–40		1.51	0.47	0.11	0.09	14.60
P3 (Semilir)	0–20	WTB	1.17	0.37	0.11	nd	15.22
	20–40		1.17	0.40	0.10	nd	14.34
P4 (Sentolo)	0–20	WLM	1.02	0.27	nd	0.04	16.07
	20–40		1.05	0.25	nd	0.04	14.98
P5 (Kebobutak)	0–20	AVM	1.28	0.36	0.22	0.10	15.67
	20–40		1.39	0.30	0.18	0.09	15.35

Note: TCS = Transported clay sediment, WVB = Weathered volcanic breccia, WTB = Weathered tuff-breccia, WLM = Weathered limestone, AVM = Altered volcanic material, nd = Not detected

clay soil (P4-Sentolo) had low values. In volcanic soils, mineralogy had a greater impact. Soils with 1:1 minerals had lower AKN and higher Si/Seq values, while soils with more 2:1 minerals had lower Si/Seq and higher AKN values.

Relationship between geochemical conditions and physicochemical properties of soil

The physicochemical properties of the soils are shown in Table 7. Particle size analysis revealed that P3-Semilir had the highest average sand fraction (29%), followed by P4-Sentolo, P5-Kebobutak, and P2-Nglanggran. P1-Wonosari exhibited the lowest average sand content (2%). Conversely, P1-Wonosari had the highest average clay content (90%), while P3-Semilir had the lowest average clay content (45%). Spearman's correlation analysis indicated a significant negative relationship between sand content and clay content ($r = -0.75$, $p < 0.05$). Sand content was also negatively correlated with CIA values ($r = -0.79$, $p < 0.01$) and VR values ($r = -0.85$, $p < 0.01$), but positively correlated with R values ($r = 0.70$, $p < 0.05$). These findings suggested that sand content in upland clay soils was associated with soil weathering intensity and the leaching of mobile elements. No significant relationship was observed between clay content and geochemical indices.

The lowest average bulk density was found in P5-Kebobutak. P3-Semilir also exhibited a relatively low average bulk density. The low bulk density in these soils was attributed to the influence of their parent materials, as volcanic ash and volcanic tuff were characterized by high porosity (Anda et al., 2016). In contrast, the average bulk density of the other soils was approximately 1.2 g cm^{-3} (Table 7). These

findings aligned with Aji et al. (2020), who reported that soils derived from volcanic ash have a lower bulk density (0.8 to 1.2 g cm^{-3}) compared to soils derived from weathered andesitic breccia (1.0 to 1.4 g cm^{-3}).

The pH H_2O values for P1-Wonosari, P2-Nglanggran, and P5-Kebobutak ranged from 5.35 to 5.93 and showed no significant differences. The highest pH H_2O was found in P4-Sentolo (8.07 to 8.18), followed by P3-Semilir (6.30 to 6.39). Soil pH varied due to differences in pedogenesis. P1-Wonosari, P2-Nglanggran, and P5-Kebobutak had lower pH values due to advanced weathering. In contrast, P4-Sentolo, derived from weathered limestone, had higher pH values as dissolved carbonates released OH^- ions into the soil solution.

The total organic matter content of the soil was also quite varied (Table 7). The total organic carbon (TOC) content in the surface layer was higher due to the accumulation of plant residues. The order of soils with the highest to lowest TOC content in the surface horizon is as follows: P5-Kebobutak > P2-Nglanggran > P4-Sentolo \approx P1-Wonosari > P3-Semilir. Furthermore, the order of TOC content in the subsurface horizon was observed as: P5-Kebobutak > P2-Nglanggran > P4-Sentolo > P3-Semilir > P1-Wonosari.

No significant differences were observed between the surface horizon and the subsurface horizon in terms of CEC values. The order of CEC values from highest to lowest is as follows: P3-Semilir > P4-Sentolo > P2-Nglanggran \approx P1-Wonosari > P5-Kebobutak. The CEC value reflects the amount of negative charge on the soil. Soil negative charges were derived from carboxylic and phenolic groups in soil organic

Table 6. Geochemical indices of the studied soils

No. Minipit (Geological formation)	Depth (cm)	Parent materials	CIA	VR	AKN	Si/Sesq	R
P1 (Wonosari)	0–20	TCS	97.15	18.82	415.02	0.25	2.32
	20–40		97.90	23.70	420.51	0.25	2.31
P2 (Nglanggran)	0–20	WVB	96.12	14.31	114.35	0.29	2.50
	20–40		96.78	15.35	132.30	0.28	2.50
P3 (Semilir)	0–20	WTB	90.48	2.78	356.92	0.35	3.12
	20–40		92.30	2.98	500.18	0.34	3.06
P4 (Sentolo)	0–20	WLM	78.10	2.09	53.83	0.31	4.07
	20–40		88.44	3.09	55.86	0.32	4.07
P5 (Kebobutak)	0–20	AVM	95.21	14.83	72.82	0.23	2.39
	20–40		97.50	22.56	117.06	0.24	2.27

Note: CIA = Chemical index of alteration, VR = Vogt residual index, AKN = Alumina to potassium oxide ratio, Si/Seq = Silica to sesquioxide, R = Ruxton ratio, TCS = Transported clay sediment, WVB = Weathered volcanic breccia, WTB = Weathered tuff-breccia, WLM = Weathered limestone, AVM = Altered volcanic material

compounds, particularly in humic substances such as humic acid, fulvic acid, humin, and hematogenic acid. However, CEC values were negatively correlated with TOC ($r = -0.76$, $p < 0.05$). The CEC values were positively correlated with CEC_{clay} values ($r = 0.77$, $p < 0.01$), indicating that the main source of negative charge in upland clay soils was the type and amount of clay minerals. In surface horizons, where organic matter accumulated, lower clay mineral content indirectly caused the negative correlation between TOC and CEC values. The high CEC values in P3-Semilir and P4-Sentolo were attributed to their considerable content of 2:1 minerals, such as smectite, which have higher CEC_{clay} values compared to 1:1 clay minerals. This was consistent with the XRD results.

Correlation analysis showed that CEC_{clay} values were positively correlated with Si/Seq ($r = 0.92$, $p < 0.01$), R ($r = 0.87$, $p < 0.01$), and sand ($r_s = 0.80$, $p < 0.01$), but negatively correlated with VR ($r = -0.93$, $p < 0.01$). These indicated that the type of clay minerals in the soils was influenced by weathering intensity and leaching of elements like Ca, Mg, and Si. The occurrence of 2:1 clay minerals was found in soils with higher R and Si/Seq values, such as P4-Sentolo and P3-Semilir.

Forms and dynamics of K and their relationships with geochemical indices and soil physicochemical properties

The concentrations of each form of K in the studied soils are presented in Table 8. Differences in parent material significantly influenced the variations in K-pseudo-total in the soils ($p < 0.001$). Significant differences in K-pseudo-total were observed among the soils, except between P1-Wonosari and P3-Semilir. The highest average K-pseudo-total was found in

P4-Sentolo (1,521 mg kg⁻¹), followed by P5-Kebobutak (927 mg kg⁻¹), P2-Nglanggran (427 mg kg⁻¹), P1-Wonosari (314 mg kg⁻¹), and P3-Semilir (264 mg kg⁻¹). Rao et al. (2011) reported K-HNO₃ + HClO₄-digest values for soils in Papua New Guinea, both volcanic and non-volcanic, ranging from 276 to 4,233 mg kg⁻¹. The K-pseudo-total values obtained in this study fall within this range.

The K_{stock} results showed a relatively similar pattern. Parent material significantly influenced variations in K_{stock} values ($p < 0.001$). No significant differences were found between P3-Kebobutak and P2-Nglanggran, or between P2-Nglanggran and P1-Wonosari. Soil depth had no significant effect on total K or K_{stock} content. Therefore, variations in K-pseudo-total and K_{stock} were mainly influenced by the parent material.

Potassium stock in upland clay soils is generally contributed by K-bearing minerals (feldspar, mica, illite, and vermiculite), organo-mineral complexes, non-exchangeable and exchangeable K, and K⁺ in soil solution (Bell et al., 2021; Jindaluang and Darunsontaya, 2023). XRD analysis showed that only P4-Sentolo contained plagioclase. However, XRF results revealed that P4-Sentolo, P3-Kebobutak, and P2-Nglanggran had higher K₂O content than other soils, suggesting that feldspar is relatively preserved in these soils. Thus, the high K-pseudo-total content in these soils is likely due to feldspar, as supported by significant correlations between K-pseudo-total and AKN values ($r_s = -0.88$, $p < 0.01$), K-lattice ($r_s = 0.77$, $p < 0.05$), and K-non-exch ($r_s = 0.69$, $p < 0.05$). AKN value, K-lattice, and K-non-exch is associated with K-bearing minerals.

The highest concentration of K-non-exch was found in P5-Kebobutak (1.58 cmolc kg⁻¹),

Table 7. Soil physicochemical properties of the studied soils

No. Minipit (Geological formation)	Depth (cm)	Sand -----	Silt (%)	Clay -----	BD (g cm ⁻³)	pH H ₂ O	TOC (g kg ⁻¹)	CEC (cmolc kg ⁻¹)	CEC _{clay}
P1 (Wonosari)	0–20	3	9	88	1.25	5.83	14.11	27.02	33.23
	20–40	1	6	93	1.28	5.51	8.70	29.04	28.93
P2 (Nglanggran)	0–20	9	20	71	1.20	5.35	15.51	28.85	42.86
	20–40	11	18	71	1.27	5.43	11.43	29.00	38.73
P3 (Semilir)	0–20	32	24	44	1.02	6.30	11.01	46.82	117.42
	20–40	25	28	47	1.09	6.39	9.47	48.65	103.58
P4 (Sentolo)	0–20	12	8	80	1.26	8.07	14.26	44.94	58.56
	20–40	11	10	79	1.26	8.18	10.21	46.47	56.65
P5 (Kebobutak)	0–20	12	29	59	0.91	5.93	19.72	18.53	32.67
	20–40	7	28	65	0.99	5.81	15.24	19.51	29.12

Note: BD = Bulk density, TOC = Total organic carbon, CEC = Cation exchange capacity, CEC_{clay} = Cation exchange capacity of clay fraction

significantly higher than in P4-Sentolo and P2-Nglanggran ($0.43 \text{ cmolc kg}^{-1}$). The lowest concentration of K-non-exch was found in P1-Wonosari ($0.15 \text{ cmolc kg}^{-1}$). The variation in K-non-exch concentrations was significantly influenced by parent material ($p < 0.01$) and soil depth ($p < 0.001$). K-non-exch concentrations were higher on the surface horizon than on the subsurface horizon for all soils.

The K-non-exch fraction includes all K forms that cannot be extracted by soil tests relying on a cation exchange mechanism and thus is characterized by slow release (Bell et al., 2021). The proportion of K-non-exch constituted 63 to 69% of the K-pseudo-total in P5-Kebobutak. This value is significantly higher compared to other clay soils (9 to 45%). The concentration of K-non-exch in P5-Kebobutak was also significantly higher than lowland clay soils in Java, which ranged from 0.44 to $0.89 \text{ cmolc kg}^{-1}$ (171 to 347 mg kg^{-1}) (Nursyamsi et al., 2008). This showed that P5-Kebobutak had a very high potential to supply K to plants through a slow-release mechanism.

The K-non-exch fraction is derived from K-bearing minerals, including weathered feldspar or mica and fixed K in the interlayer spaces of phyllosilicate minerals (Bell et al., 2021). The concentration of K-non-exch was linked to weathered feldspar, as indicated by a negative relationship between K-non-exch and the AKN value ($r = -0.79$, $p < 0.01$). Higher AKN values indicated fewer weathered feldspar, leading to

lower K-non-exch concentrations in upland clay soils.

Nitric acid was known to break down mineral structures, with some K-non-exch extracted from the interlayers of primary micas and feldspar interiors. However, P4-Sentolo, which had similar K_2O and AKN values to P5-Kebobutak, showed a much lower K-non-exch concentration (Table 6). This lower concentration was likely due to the dilution effect of CaCO_3 , as observed in soils rich in free carbonate (Zareian et al., 2018). P4-Sentolo contained free carbonates ranging from 3.69 to 20.21% (data not shown).

A positive correlation was observed between K-non-exch and TOC ($r = 0.88$, $p < 0.01$). Higher K-non-exch concentrations in the surface horizon were attributed to organic matter accumulation. Stable organic carbon, protected K-bearing minerals and reduced their solubility (Rosenstock et al., 2019; Jindaluang and Darunsontaya, 2023). Consequently, feldspars weathering occurred more slowly, leading to a low AKN value. The acid extraction method used in this study was strong enough to dissolve K, not only in feldspars but also in organo-mineral complexes (Rosenstock et al., 2019).

The high concentration of K-non-exch in P5-Kebobutak, compared to other soils, was attributed to its low AKN value and high TOC content. This condition led to the formation of organic matter coatings on feldspar, which protected it from weathering and contributed to the increased K-non-exch concentration.

Table 8. Forms of K in the studied clay soils

Profile No. (Location)	Depth (cm)	Parent materials	K-Fraction				K_{stock} (ton ha^{-1})	
			K-pseudo- total ----- (mg kg^{-1})	K- lattice -----	K- exch (cmolc kg^{-1})	K-non exch (cmolc kg^{-1})		K-water- sol (mg kg^{-1})
P1 (Wonosari)	0–20	TCS	328 ^d	217 ^{cd}	0.09 ^{cd}	0.19 ^{ab}	3.37 ^b	0.83 ^c
	20–40		299 ^d	237 ^{cd}	0.04 ^e	0.11 ^{bb}	3.61 ^b	0.75 ^c
P2 (Nglanggran)	0–20	WVB	414 ^c	88 ^e	0.33 ^a	0.48 ^{aa}	10.70 ^a	1.01 ^{bc}
	20–40		439 ^c	219 ^{cd}	0.17 ^b	0.37 ^{ba}	7.70 ^a	1.10 ^{bc}
P3 (Semilir)	0–20	WTB	260 ^d	110 ^{de}	0.12 ^{bc}	0.26 ^{ab}	4.27 ^{bc}	0.54 ^d
	20–40		267 ^d	189 ^{cde}	0.05 ^{de}	0.14 ^{bb}	4.20 ^{bc}	0.57 ^d
P4 (Sentolo)	0–20	WLM	1,326 ^a	1,092 ^b	0.14 ^{bc}	0.45 ^{aa}	4.89 ^b	3.23 ^a
	20–40		1,715 ^a	1,524 ^a	0.07 ^{cd}	0.41 ^{ba}	2.56 ^b	4.47 ^a
P5 (Kebobutak)	0–20	AVM	1,007 ^b	246 ^c	0.14 ^{bc}	1.78 ^{aa}	11.30 ^{ab}	1.86 ^b
	20–40		847 ^b	204 ^{cde}	0.21 ^{ab}	1.37 ^{ba}	21.90 ^{ab}	1.62 ^b
Depth (D)			0.775	0.001	< 0.001	0.001	0.459	0.643
Parent material (PM)			< 0.001	< 0.001	< 0.001	< 0.001	0.049	< 0.001
D><PM			0.945	< 0.001	0.025	0.324	0.774	0.957

Note: TCS = Transported clay sediment, WVB = Weathered volcanic breccia, WTB = Weathered tuff-breccia, WLM = Weathered limestone, AVM = Altered volcanic material

Furthermore, the accumulation of organic matter resulted in a higher proportion of aggregates > 2 mm in the soil. Recent studies have shown that the potential to accumulate the K-non-exch fraction was greater in aggregates > 2 mm than in smaller aggregates (Kai-lou et al., 2022). P5-Kebobutak also exhibited the highest porosity and macro-aggregate content among the studied soils (data not shown), which can be attributed to both the nature of its parent material and the presence of organic matter.

K-lattice refers to K^+ that has been incorporated into the interlayer spaces of 2:1 minerals and dehydrated, becoming part of the mineral structure (Bell et al., 2021). This fraction of K can only be released into the soil solution through weathering and is difficult to utilize for agronomic purposes (Han et al., 2019; Soumare et al., 2023). The highest average K-lattice concentration was found in P4-Sentolo (1,308 mg kg⁻¹), significantly exceeding the concentration in P1-Wonosari (227 mg kg⁻¹) and P5-Kebobutak (225 mg kg⁻¹). The lowest K-lattice concentration was observed in P3-Semilir (150 mg kg⁻¹) and P2-Nglanggran (154 mg kg⁻¹). Additionally, all soils exhibited higher K-lattice in the subsurface horizon compared to the surface horizon. Significant differences in K-lattice concentration were influenced by the interaction between parent material and soil horizon ($p < 0.001$).

The high K-lattice content indicated the presence of reactive 2:1 minerals, such as illite, interstratified illite/mica, and vermiculite, which are known to fix K (Portela et al., 2019). However, the bulk sample analysis did not reveal the presence of these minerals in any of the soils studied. Thus, the K-lattice content in this study was likely associated with weathered feldspars. The notably high K-lattice content in P4-Sentolo, compared to other soils, was attributed to the low concentration of K-non-exch in that soil, which was influenced by the dilution effect of CaCO₃. As a result, the K-lattice concentration, determined by the difference between K-pseudo-total and other forms of K, was elevated. No correlation was found between the geochemical indices, physicochemical properties, or other K forms with the K-lattice content. The lack of correlation between K-lattice and K-non-exch suggested that K-lattice was a stable form that did not significantly contribute to the K equilibrium in the soil.

The proportion of K-lattice to K-pseudo-total varied across the soils, ranging from 82 to 89% in

P4-Sentolo, 66 to 79% in P1-Wonosari, 42 to 71% in P3-Semilir, 21 to 50% in P2-Nglanggran, and 24% in P5-Kebobutak. These proportions indicated that K in P4-Sentolo was almost entirely in the form of K-lattice, suggesting that the K in this soil was largely unavailable for agronomic purposes. A similar pattern was observed in P1-Wonosari and P3-Semilir. In contrast, the lower proportion of K-lattice in P2-Nglanggran and P5-Kebobutak indicated that the K in these soils was not fixed by minerals, making it potentially available for plant utilization.

The concentration of K-exch in all soils was influenced by the interaction between parent material and soil depth ($p < 0.05$). P2-Nglanggran exhibited the highest average concentration of K-exch (0.25 cmolc kg⁻¹), followed by P5-Kebobutak (0.18 cmolc kg⁻¹) and P4-Sentolo (0.11 cmolc kg⁻¹). Statistically, the concentrations of K-exch in these three soils were not significantly different. The lowest concentration was found in P1-Wonosari (0.06 cmolc kg⁻¹), followed by P3-Semilir (0.08 cmolc kg⁻¹). The range of K-exch concentrations in this study was broader than that reported for lowland clay soils of Java Island, which range from 0.13 to 0.25 cmolc kg⁻¹ (50 to 99 mg kg⁻¹) (Nursyamsi et al., 2008). In most soils, the concentration of K-exch in the surface horizon was higher than in the subsurface horizon, except for P5-Kebobutak.

From all fractions, K-water-sol has the smallest proportion, which accounted for 0.1 to 2.6% of the K-pseudo-total. P5-Kebobutak exhibited the highest average concentration of K-water-sol (16.60 mg kg⁻¹), followed by P2-Nglanggran (9.20 mg kg⁻¹). Other soils contained relatively low concentrations of K-water-sol (2.56 to 4.89 mg kg⁻¹). The variation in K-water-sol concentration among soils was influenced by parent material ($p < 0.05$), but no significant effect of soil depth was observed.

A positive correlation was found between K-exch and K-water-sol ($r = 0.83$, $p < 0.01$) and between K-exch and K-non-exch ($r = 0.78$, $p < 0.01$). These findings indicated that K forms in clay soils were dynamically related, with one form influencing the others. The results suggested an equilibrium among K forms, where a decrease in one form was balanced by the others (Pathariya et al., 2022).

No significant relationship was found between K-exch or K-water-sol and CEC or clay content. This was unexpected, as plant-available K (K-exch and K-water-sol) is usually associated with the negative charge of clay minerals

(Nursyamsi et al., 2008; Han et al., 2019; Bell et al., 2021). Unlike K-non-exch, no correlation was found between K-exch and K-water-sol with geochemical indices. Soil weathering and mineralogy did not significantly influence plant-available K. Instead, a positive correlation with TOC was identified, emphasizing the role of organic carbon in releasing K^+ into the soil solution in upland clay soils.

Jindaluang and Darunsontaya (2023) reported a positive relationship between K-non-exch, K-exch, and K-water-sol with stable organic carbon forms, such as carboxyl and aromatic carbon, in Mollisols and Vertisols under irrigation. They explained that K^+ availability and retention increased due to the formation of complexes between minerals and stable organic fractions. This process was found to enhance non-exchangeable and exchangeable K in clay soils. In this study, P5-Kebobutak and P3-Nglanggran showed relatively higher levels of plant-available K compared to other soils. Their high TOC content was the main factor contributing to the increased availability of K. The high availability of K in these soils likely resulted from organic residue decomposition, which formed organo-mineral complexes. Additionally, these soils contained higher proportions of K-non-exch compared to the others. Enhancing plant-available K in clay soils should focus on the cycling and input of organic matter. Retaining crop residues through long-term conservation agriculture has been shown to enhance and sustain K supply to crops (Rani et al., 2023).

Based on the critical cation deficiency status (CCDS) for tropical soils, the critical threshold for K-exch concentration is between 0.4 and 0.5 cmolc kg^{-1} (Soil Research Center, 1983). It is

important to note that the critical concentration varies among plant species. Using the lower limit of 0.4 cmolc kg^{-1} , all soils in this study were classified as deficient in K. Therefore, K fertilization is essential for agricultural cultivation. Low K availability can reduce crop productivity, as reported by Rizzo et al. (2024).

In addition to the low K concentration, cation saturation at the exchange complex also requires attention. The K-exch concentration was consistently lower than Na-exch in most soils, except for P2-Nglanggran (Table 9). Cation imbalances were observed in P3-Semilir and P4-Sentolo, where the combined saturation of Ca^{2+} plus Mg^{2+} saturation exceeded 100%. This imbalance has the potential to disrupt the K^+ balance in the exchange complex. Correlation analysis showed a negative relationship between Ca-exch and K-water-sol ($r = -0.79$, $p < 0.01$). Additionally, studies by Leikemarian et al. (2018) and Hailu et al. (2015) reported K deficiencies in soils with high Mg-exch concentrations, as Mg competes with K at exchange sites.

Since the contribution of K-non-exch varies among soils, K fertilization in clay soils must be carefully managed. Both K-non-exch and K-exch should be considered when assessing soil K availability. P5-Kebobutak, with its high K-non-exch concentration, provides a long-term K supply through slow release, reducing the need for frequent fertilization. For annual crops, K fertilization may only be required during early growth stages. In contrast, P1-Wonosari, P2-Nglanggran, P3-Semilir, and P4-Sentolo are unlikely to supply K in the long term, requiring periodic fertilization. Additionally, continuous application of organic materials is necessary in all upland clay soils to maintain K^+ availability.

Table 9. Concentrations of exchangeable cations of the studied clay soils

No. Minipit (Geological formation)	Depth (cm)	Parent materials	Ca^{2+} -exch -----	Mg^{2+} -exch (cmolc kg^{-1})	K^+ -exch -----	Na^+ -exch -----
P1 (Wonosari)	0–20	TCS	12.07	2.34	0.09	0.14
	20–40		9.85	1.66	0.04	0.11
P2 (Nglanggran)	0–20	WVB	6.71	2.35	0.33	0.11
	20–40		6.80	2.33	0.17	0.12
P3 (Semilir)	0–20	WTB	32.28	18.78	0.12	0.20
	20–40		30.91	19.44	0.05	0.19
P4 (Sentolo)	0–20	WLM	71.71	1.96	0.14	0.20
	20–40		75.84	2.23	0.07	0.21
P5 (Kebobutak)	0–20	AVM	6.41	1.88	0.14	0.32
	20–40		5.13	1.79	0.21	0.32

Note: TCS = Transported clay sediment, WVB = Weathered volcanic breccia, WTB = Weathered tuff-breccia, WLM = Weathered limestone, AVM = Altered volcanic material

CONCLUSIONS

This study highlighted the influence of parent materials, mineralogy, and organic carbon on K dynamics in the upland clay soils of Yogyakarta. Although feldspar was not identified by XRD analysis, geochemical data suggest its significant contribution to K-pseudo-total, K_{stock} , and K-non-exch concentrations. P5-Kebobutak exhibited the highest K-non-exch concentration, providing a long-term K source through slow release. Both K-exch and K-water-sol concentrations showed significant correlations with TOC and K-non-exch, but not with geochemical indices. All soils were classified as K-deficient, indicating the need for targeted fertilization strategies considering both K-exch and K-non-exch. Furthermore, the application of organic amendments is essential for enhancing K availability.

ACKNOWLEDGEMENT

The authors would like to express their gratitude to Mr. Nurfatoni for his assistance with the soil analysis and to the Research Directorate of Universitas Gadjah Mada for providing funds to support this research through the Academic Excellence A Program (contract no.: 2490/UN1/DITLIT/Dit-Lit/PT.01.07/2023).

REFERENCES

- Aji, K., Maas, A., & Nurudin, M. (2020). Relationship between soil morphology and variability of upland degradation in Bogowonto Watershed, Central Java, Indonesia. *Journal of Degraded and Mining Lands Management*, 7(3), 2209–2219. <https://doi.org/10.15243/jdmlm.2020.073.2209>
- Akbas, F., Gunal, H., & Acir, N. (2017). Spatial variability of soil potassium and its relationship to land use and parent material. *Soil and Water Research*, 12(4), 202–211. <https://dx.doi.org/10.17221/32/2016-SWR>
- Anda, M., Suparto, & Sukarman. (2016). Characteristics of pristine volcanic materials: Beneficial and harmful effects and their management for restoration of agroecosystem. *Science of The Total Environment*, 543, 480–492. <https://doi.org/10.1016/j.scitotenv.2015.10.157>
- Anda, M., Suryani, E., & Subardja, D. (2015). Strategy to reduce fertilizer application in volcanic paddy soils: Nutrient reserves approach from parent materials. *Soil and Tillage Research*, 150, 10–20. <https://doi.org/10.1016/j.still.2015.01.005>
- Babla, M. H., Donovan-Mak, M., Cazzonelli, C. I., Tissue, D. T., & Chen, Z. H. (2023). Linking high light-induced cellular ionic and oxidative responses in leaves to fruit quality in tomato. *Plant Growth Regulation*, 101(1), 267–84. <https://doi.org/10.1007/s10725-023-01018-9>
- BBSDLP. (2017a). *Atlas peta tanah semi detail skala 1:50.000, Kabupaten Bantul, Provinsi Daerah Istimewa Yogyakarta*. Bogor, Indonesia: Research and Development of Agricultural Land Resources Center, Ministry of Agriculture.
- BBSDLP. (2017b). *Atlas peta tanah semi detail skala 1:50.000, Kabupaten Sleman, Provinsi Daerah Istimewa Yogyakarta*. Bogor, Indonesia: Research and Development of Agricultural Land Resources Center, Ministry of Agriculture.
- Bell, M. J., Ransom, M. D., Thompson, M. L., Hinsinger, P., Florence, A. M., Moody, P. W., & Guppy, C. N. (2021). Considering soil potassium pools with dissimilar plant availability. *Improving potassium recommendations for agricultural crops*, pp. 163–190. Springer. https://doi.org/10.1007/978-3-030-59197-7_7
- Butler, B. M., Palarea-Albaladejo, J., Shepherd, K. D., Nyambura, K. M., Towett, E. K., Sila, A. M., & Hillier, S. (2020). Mineral–nutrient relationships in African soils assessed using cluster analysis of X-ray powder diffraction patterns and compositional methods. *Geoderma*, 375, 114474. <https://doi.org/10.1016/j.geoderma.2020.114474>
- Demidchik, V., Straltsova, D., Medvedev, S. S., Pozhvanov, G. A., Sokolik, A., & Yurin, V. (2014). Stress-induced electrolyte leakage: The role of K^+ -permeable channels and involvement in programmed cell death and metabolic adjustment. *Journal of experimental botany*, 65(5), 1259–1270. <https://doi.org/10.1093/jxb/eru004>
- Enang, R. K., Yerima, B. P. K., Kome, G. K., & Van Ranst, E. (2020). Soil physicochemical properties and geochemical indices: Diagnostic tools for evaluating pedogenesis in tephra-derived soils along the Cameroon volcanic line. *Eurasian Soil Science*, 53(8),

- 1079–1099. <https://doi.org/10.1134/s1064229320080050>
- Fiantis, D., Ginting, F. I., Halfero, F., Saputra, A. P., Nelson, M., Van Ranst, E., & Minasny, B. (2021). Geochemical and mineralogical composition of the 2018 volcanic deposits of Mt. Anak Krakatau. *Geoderma Regional*, 25, e00393. <https://doi.org/10.1016/j.geodrs.2021.e00393>
- Fiantis, D., Malone, B., Pallasser, R., Van Ranst, E., & Minasny, B. (2017). Geochemical fingerprinting of volcanic soils used for wetland rice in West Sumatra, Indonesia. *Geoderma Regional*, 10, 48–63. <https://doi.org/10.1016/j.geodrs.2017.04.004>
- Hailu, H., Mamo, T., Keskinen, R., Karlun, E., Gebrekidan, H., & Bekele, T. (2015). Soil fertility status and wheat nutrient content in Vertisol cropping systems of central highlands of Ethiopia. *Agriculture & Food Security*, 4(1), 19. <https://doi.org/10.1186/s40066-015-0038-0>
- Han, T., Huang, J., Liu, K., Fan, H., Shi, X., Chen, J., ..., & Huimin, Z. (2021). Soil potassium regulation by changes in potassium balance and iron and aluminum oxides in paddy soils subjected to long-term fertilization regimes. *Soil and Tillage Research*, 214, 105168. <https://doi.org/10.1016/j.still.2021.105168>
- Han, G.-Z., Huang, L.-M., & Tang, X.-G. (2019). Potassium supply capacity response to K-bearing mineral changes in Chinese purple paddy soil chronosequences. *Journal of Soils and Sediments*, 19(3), 1190–1200. <https://doi.org/10.1007/s11368-018-2124-y>
- Han, T., Liu, K., Huang, J., Khan, M. N., Shen, Z., Li, J., & Zhang, H. (2023). Temporal and spatial characteristics of paddy soil potassium in China and its response to organic amendments: A systematic analysis. *Soil and Tillage Research*, 235, 105894. <https://doi.org/10.1016/j.still.2023.105894>
- Harnois, L., & Moore, J. M. (1988). Geochemistry and origin of the Ore Chimney Formation, a transported paleoregolith in the Grenville Province of southeastern Ontario, Canada. *Chemical Geology*, 69(3–4), 267–289. [https://doi.org/10.1016/0009-2541\(88\)90039-3](https://doi.org/10.1016/0009-2541(88)90039-3)
- Harsha, B. R., & Jagadeesh, B. R. (2017). Studies on distribution of potassium fraction in surface and sub-surface layers of black soils. *Journal of Pharmacognosy and Phytochemistry*, 6(6), 2596–2601. Retrieved from <https://www.phytojournal.com/archives/2017.v6.i6.2494/studies-on-distribution-of-potassium-fraction-in-surface-and-sub-surface-layers-of-black-soils>
- Hasanuzzaman, M., Bhuyan, M. H., Nahar, K., Hossain, M. S., Mahmud, J. A., Hossen, M. S., Masud, A. A., & Fujita, M. (2018). Potassium: A vital regulator of plant responses and tolerance to abiotic stresses. *Agronomy*, 8(3), 31. <https://doi.org/10.3390/agronomy8030031>
- Heidari, A., Osat, M., & Konyushkova, M. (2022). Geochemical indices as efficient tools for assessing the soil weathering status in relation to soil taxonomic classes. *CATENA*, 208, 105716. <https://doi.org/10.1016/j.catena.2021.105716>
- Irawan, W., & Putra, E. T. S. (2020). The effect of potassium addition on oil palm (*Elaeis guineensis* Jacq.) root anatomic properties under drought stress. *Caraka Tani: Journal of Sustainable Agriculture*, 35(1), 54–65. <http://dx.doi.org/10.20961/carakatani.v35i1.32578>
- Jindaluang, W., & Darunsontaya, T. (2024). Role of soil organic carbon composition on potassium availability in smectite-dominated paddy soils. *Journal of Soil Science and Plant Nutrition*, 24, 1288–1300. <https://doi.org/10.1007/s42729-024-01631-1>
- Kai-lou, L., Jing, H., Tian-fu, H., Ya-zhen, L., Dong-chu, L., Qaswar, M., ..., & Hui-min, Z. (2022). The relationship between soil aggregate-associated potassium and soil organic carbon with glucose addition in an Acrisol following long-term fertilization. *Soil and Tillage Research*, 222, 105438. <https://doi.org/10.1016/j.still.2022.105438>
- Kauer, K., Pärnpuu, S., Talgre, L., Eremeev, V., & Luik, A. (2021). Soil particulate and mineral-associated organic matter increases in organic farming under cover cropping and manure addition. *Agriculture*, 11(9), 903. <https://doi.org/10.3390/agriculture11090903>
- Kitagawa, Y., Yanai, J., & Nakao, A. (2018). Evaluation of non-exchangeable potassium content of agricultural soils in Japan by the boiling HNO₃ extraction method in comparison with exchangeable potassium.

- Soil Science and Plant Nutrition*, 64(1), 116–122. <https://doi.org/10.1080/00380768.2017.1411168>
- Kome, G. K., Enang, R. K., Tabi, F. O., & Yerima, B. P. K. (2019). Influence of clay minerals on some soil fertility attributes: A review. *Open Journal of Soil Science*, 09(09), 155–188. <https://doi.org/10.4236/ojss.2019.99010>
- Kowalska, J. B., Skiba, M., Maj-Szeliga, K., Mazurek, R., & Zaleski, T. (2021). Does calcium carbonate influence clay mineral transformation in soils developed from slope deposits in Southern Poland? *Journal of Soils and Sediments*, 21(1), 257–280. <https://doi.org/10.1007/s11368-020-02764-3>
- Laekemariam, F., Kibret, K., & Shiferaw, H. (2018). Potassium (K)-to-magnesium (Mg) ratio, its spatial variability and implications to potential Mg-induced K deficiency in Nitisols of Southern Ethiopia. *Agriculture & Food Security*, 7(1), 13. <https://doi.org/10.1186/s40066-018-0165-5>
- Maier, C. R., Chen, Z. H., Cazzonelli, C. I., Tissue, D. T., & Ghannoum, O. (2022). Precise phenotyping for improved crop quality and management in protected cropping: A review. *Crops*, 2(4), 336–50. <https://doi.org/10.3390/crops2040024>
- Moignien, R. (1966). *Review of research on laterites*. Paris: United Nations Educational, Scientific and Cultural Organisation. Retrieved from <https://unesdoc.unesco.org/ark:/48223/pf0000071101>
- Mulyanto, D. (2020). Material vulkanik sebagai penyusun utama tanah merah di atas batuan karbonat Karang Sari Wonosari. *Jurnal Tanah dan Air*, 17(2), 45–55. <https://doi.org/10.31315/jta.v17i2.4234>
- Navarro-Hasse, E., Yáñez, C., Neaman, A., & Pinochet, D. (2023). The effects of parent rock on soil clay mineralogy and soil physicochemical properties: A review. *Idesia (Arica)*, 41(4), 125–139. <https://doi.org/10.4067/S0718-34292023000400125>
- Négre, P., Ladenberger, A., Reimann, C., Demetriades, A., Birke, M., & Sadeghi, M. (2023). GEMAS: Chemical weathering of silicate parent materials revealed by agricultural soil of Europe. *Chemical Geology*, 639, 121732. <https://doi.org/10.1016/j.chemgeo.2023.121732>
- Nesbitt, H. W., & Young, G. M. (1984). Prediction of some weathering trends of plutonic and volcanic rocks based on thermodynamic and kinetic considerations. *Geochimica et Cosmochimica Acta*, 48(7), 1523–1534. [https://doi.org/10.1016/0016-7037\(84\)90408-3](https://doi.org/10.1016/0016-7037(84)90408-3)
- Nursyamsi, D., Idris, K., Sabiham, S., Rachim, D., & Sofyan, A. (2008). Dominant soil characteristics influencing available potassium on smectitic soils. *Indonesian Journal of Agriculture*, 1(2), 121–131. Retrieved from <https://repository.pertanian.go.id/server/api/core/bitstreams/444bbfd2-b2a5-4dcf-b825-dbd257d6cfd4/content>
- Pathariya, P., Dwivedi, B. S., Dwivedi, A. K., Thakur, R. K., Singh, M., & Sarvade, S. (2022). Potassium balance under soybean–wheat cropping system in a 44 year old long term fertilizer experiment on a Vertisol. *Communications in Soil Science and Plant Analysis*, 53(2), 214–226. <https://doi.org/10.1080/00103624.2021.1984516>
- Portela, E., Monteiro, F., Fonseca, M., & Abreu, M. M. (2019). Effect of soil mineralogy on potassium fixation in soils developed on different parent material. *Geoderma*, 343, 226–234. <https://doi.org/10.1016/j.geoderma.2019.02.040>
- Pulungan, N. A., & Sartohadi, J. (2018). New approach to soil formation in the transitional landscape zone: Weathering and alteration of parent rocks. *Journal of Environments*, 5(1), 1–7. <https://doi.org/10.20448/journal.505.2018.51.1.7>
- R Core Team. (2020). *R: A language and environment for statistical computing*. Vienna, Austria: R Foundation for Statistical Computing. Retrieved from <https://cran.r-project.org/doc/manuals/r-release/fullrefman.pdf>
- Rahardjo, W., Sukandarrumidi, & Rosidi, H. M. D. (1995). *Peta geologi lembar Yogyakarta skala 1:100.000*. Bandung: Geological Research and Development Center. Retrieved from <https://geologi.esdm.go.id/geomap/pages/preview/peta-geologi-lembar-kebumen-jawa>
- Rani, K., Datta, A., Jat, H., Choudhary, M., Sharma, P., & Jat, M. (2023). Assessing the availability of potassium and its quantity–intensity relations under long term

- conservation agriculture based cereal systems in North-West India. *Soil and Tillage Research*, 228, 105644. <https://doi.org/10.1016/j.still.2023.105644>
- Rao, B. R., Bailey, J., & Wingwafi, R. W. (2011). Comparison of three digestion methods for total soil potassium estimation in soils of Papua New Guinea derived from varying parent materials. *Communications in soil science and plant analysis*, 42(11), 1259–1265. <http://dx.doi.org/10.1080/00103624.2011.571740>
- Rawat, J., Sanwal, P., & Saxena, J. (2016). Potassium and its role in sustainable agriculture. *Potassium solubilizing microorganisms for sustainable agriculture* (pp. 235–253). New Delhi: Springer India. https://doi.org/10.1007/978-81-322-2776-2_17
- Rizzo, G., Agus, F., Susanti, Z., Buresh, R., Cassman, K. G., Dobermann, A., ..., & Grassini, P. (2024). Potassium limits productivity in intensive cereal cropping systems in Southeast Asia. *Nature Food*, 5(11), 929–938. <https://doi.org/10.1038/s43016-024-01065-z>
- Roadset, E. (1972). Mineralogy and geochemistry of quaternary clays in the Numedal Area, southern Norway. *Norsk Geolisk Tidsskrift*, 52, 335–369. Retrieved from https://foreninger.uio.no/ngf/ngt/pdfs/NGT_52_4_335-369.pdf
- Rosenstock, N. P., Stendahl, J., Van Der Heijden, G., Lundin, L., Mcgivney, E., Bishop, K., & Löfgren, S. (2019). Base cations in the soil bank: Non-exchangeable pools may sustain centuries of net loss to forestry and leaching. *SOIL*, 5(2), 351–366. <https://doi.org/10.5194/soil-5-351-2019>
- Ruxton, B. P. (1968). Measures of the degree of chemical weathering of rocks. *The Journal of Geology*, 76(5), 518–527. <https://doi.org/10.1086/627357>
- Sardans, J., & Peñuelas, J. (2021). Potassium control of plant functions: Ecological and agricultural implications. *Plants*, 10(2), 419. <https://doi.org/10.3390/plants10020419>
- Sartohadi, J., Harlin Jennie Pulungan, N. A., Nurudin, M., & Wahyudi, W. (2018). The ecological perspective of landslides at soils with high clay content in the middle Bogowonto Watershed, Central Java, Indonesia. *Applied and Environmental Soil Science*, 2018(1), 2648185. <https://doi.org/10.1155/2018/2648185>
- Soil Research Center. (1983). *Terms of Reference. Soil Capability Survey*. Soil Research Center: Department of Agriculture No.59/1983.
- Soumare, A., Sarr, D., & Diédhiou, A. G. (2023). Potassium sources, microorganisms and plant nutrition: Challenges and future research directions. *Pedosphere*, 33(1), 105–115. <https://doi.org/10.1016/j.pedsph.2022.06.025>
- Surono, Toha B., & Sudarno I. (1992). *Peta geologi lembar Surakarta-Giritontro skala 1:100.000*. Bandung: Geological Research and Development Center. Retrieved from <https://geologi.esdm.go.id/geomap/pages/preview/peta-geologi-lembar-yogyakarta-jawa>
- Tavares, T. R., Nunes, L. C., Alves, E. E., Almeida, E. D., Maldaner, L. F., Krug, F. J., Carvalho, H. W., & Molin, J. P. (2018). Simplifying sample preparation for soil fertility analysis by X-ray fluorescence spectrometry. *Sensors*, 19(23), 5066. <https://doi.org/10.3390/s19235066>
- Temga, J. P., Sababa, E., Mamdem, L. E., Bijeck, M. L. N., Azinwi, P. T., Tehna, N., ..., & Ndjigui, P. (2021). Rare earth elements in tropical soils, Cameroon soils (Central Africa). *Geoderma Regional*, 25, e00369. <https://doi.org/10.1016/j.geodrs.2021.e00369>
- Underwood, D. S., Yurchenko, S. N., Tennyson, J., & Jensen, P. (2014). Rotational spectrum of SO₃ and theoretical evidence for the formation of sixfold rotational energy-level clusters in its vibrational ground state. *The Journal of Chemical Physics*, 140(24), 244316. <https://doi.org/10.1063/1.4882865>
- van Reeuwijk, L. P. (2002). *Soil testing methods*. Global Soil Doctors Programme. Food and Agriculture Organization of the United Nations. Rome. Retrieved from <https://www.isric.org/documents/document-type/technical-paper-09-procedures-soil-analysis-6th-edition>
- Van Reeuwijk, L. P. (2002). *Technical paper 09: Procedures for soil analysis*. International Soil Reference and Information Centre, Food and Agriculture Organization of the United Nations. Retrieved from https://www.isric.org/sites/default/files/ISRIC_TechPap09.pdf

- Volf, M. R., Benites, V. M., Azevedo, A. C., Moraes, M. F., Tiritan, C. S., & Rosolem, C. A. (2023). Soil mineralogy and K reserves in soils from the Araguaia River valley, Brazil. *Geoderma Regional*, 33, e00654. <https://doi.org/10.1016/j.geodrs.2023.e00654>
- Zareian, G., Farpoor, M. H., Hejazi-Mehrizi, M., & Jafari, A. (2018). Kinetics of non-exchangeable potassium release in selected soil orders of southern Iran. *Soil and Water Research*, 13(4), 200–207. <https://doi.org/10.17221/138/2017-swr>
- Zörb, C., Senbayram, M., & Peiter, E. (2014). Potassium in agriculture – Status and perspectives. *Journal of Plant Physiology*, 171(9), 656–669. <https://doi.org/10.1016/j.jplph.2013.08.008>